

## Origin of the low-frequency modes of globular proteins

Simone Melchionna \*

*INFM and Dipartimento di Fisica, Università "La Sapienza," Piazza Aldo Moro, 5, 00185 Rome, Italy*

Alessandro Desideri †

*INFM and Dipartimento di Biologia, Università "Tor Vergata," via della Ricerca Scientifica, 00133 Rome, Italy*

(Received 22 October 1998; revised manuscript received 30 April 1999)

The incoherent structure factor associated with the nonexchangeable hydrogen atoms of carbomonoxy myoglobin at 80 and 200 K in a solvated sample has been computed from molecular dynamics simulations. The evaluated mean square displacements are almost three times larger than the experimental ones. However, the low-frequency band centered at 3 meV, observed in neutron scattering experiments, is reproduced. Evaluation of the contribution to the spectrum from different protein shells and backbone and side chain atoms allows us to propose that the low-frequency mode around 3 meV, which is a constant feature of all globular proteins, is mainly due to the hydrogen atoms belonging to the inner shell, suggesting that this mode is intrinsic to the protein itself. [S1063-651X(99)14110-2]

PACS number(s): 87.15.-v, 87.14.Ee

### I. INTRODUCTION

Evidence of the existence of low-frequency motions in proteins in the picosecond time scale has been provided either by experiments or by simulative methods such as molecular dynamics (MD) and normal mode analysis. Indication of a low-frequency band came from Raman experiments, which were able to detect a broad maximum at 3.7 meV on a liophylized chymotrypsin sample [1]. A peak at about 3.1 meV was then observed again with Raman spectroscopy on several globular proteins [2] and was confirmed by neutron scattering experiments on polycrystalline lysozyme [3]. Actually, inelastic neutron scattering is a very accurate tool to investigate atomic dynamics in the pico and nanosecond time scale, probing both vibrational and diffusive motions. Inelastic neutron scattering data collected at low temperatures have shown the presence of a similar spectrum, characterized by a broad maximum in the incoherent dynamic structure factor at around 3.0 meV in trypsin inhibitor, myoglobin (Mb), hemoglobin, lysozyme, and even red blood cells [4–6]. At room temperature this band is buried by a strong quasielastic scattering. The origin of the low-frequency band at around 3 meV, which has been evidenced also in the far infrared transmission spectrum of dry lysozyme using synchrotron radiation [7], is not yet well understood.

In the past the protein low-frequency spectrum has been interpreted as the overlap of the vibrational motion of an elastic sphere with characteristic frequencies inversely proportional to the radius of the sphere [9,10] although this dependence has not been confirmed experimentally [2]. Later on, it has been suggested that the low-frequency modes could be related to accordionlike modes of  $\alpha$  helices in the

secondary structure of proteins [11] and their frequencies have been calculated for several proteins in the 2.4–3.7-meV range.

A recent inelastic scattering study in the low-frequency range of deuterated myoglobin and lysozyme at full and low hydration has suggested that the band at around 3 meV is mostly contributed by water-coupled librations of the side chain groups, in particular, the polar ones that are depressed in the hydrated sample by strong hydrogen bond interactions [12].

In this context, MD simulations performed on Mb were able to qualitatively reproduce the inelastic peak [13,14], although the peak was systematically shifted to lower frequencies by a factor ranging from 2 to 3. Possible explanations to this discrepancy have been suggested as the use of an inaccurate simulation model (force field), or the different boundary conditions of the experimental and the simulation samples. In fact, the experiments are usually achieved on protein crystal powders with a certain amount of hydration water, while the simulations are usually performed on a solution at virtually high concentration. Moreover, a strong dependence of the inelastic peak with the treatment of electrostatics has been observed [14], in particular, concerning the use of different truncated models to compute the electrostatic interactions. It was noted that the same MD simulations used to investigate the atomic fluctuations of Mb versus temperature were able to reproduce qualitatively the glasslike transition of Mb, but the atomic Debye-Waller factors computed at low temperatures exhibited values systematically larger than the experimental ones, by a factor of 2 to 3, i.e., the same ratio observed for the shift in frequency.

In this paper we have simulated a solvated myoglobin sample in the isothermal-isobaric ensemble and treated the electrostatics with the Ewald summation method. The dynamic structure factors calculated in this way are found to match in shape and energy the experimental data. However the mean square displacements are still 2–3 times larger than the measured ones probably for the inaccuracy of the force field [15].

\*Present address: Department of Chemistry, University of Cambridge, Lensfield Road, Cambridge CB2 1EW, United Kingdom.

†Author to whom correspondence should be addressed. Electronic address: [desideri@uniroma2.it](mailto:desideri@uniroma2.it)

Analysis of our trajectories by considering the contribution to the incoherent dynamic structure factor of selected protons located in specific parts of the protein allows us to observe that the low-frequency band observed in globular proteins is due to a dominant role of the side chain groups that are not necessarily located in the external part of the protein. Our results allow us to reinterpret the observed line shapes in terms of protein intrinsic motions modulated by the interaction with the solvent.

## II. COMPUTATIONAL METHODS

All MD simulations discussed in this paper have been performed by using the program DL\_PROTEIN [16], a fully parallel MD code suited to simulate biological molecules. Runs have been achieved on the parallel Origin 2000 and T3E platforms of Cineca (Bologna, Italy).

We have simulated a carbomonoxy myoglobin protein embedded in 1513 water molecules plus 9 chlorine counterions. The adopted force field is the Charmm22 scheme [17] by treating all atoms of the protein including aliphatic, i.e., nonexchangeable, hydrogen atoms explicitly. Each atom carries a Van der Waals interaction term with the Lorentz-Berthelot rules adopted to handle interatomic interactions, plus a partial charge. The Hamiltonian also presents bond angle and dihedral potential terms, plus a redefined Van der Waals interaction term on the short-range topological distance, in order to mime at best the chemical bonding. The water molecules have been treated with the TIP3P water model, as it is used in the Charmm22 parameter set.

The full connectivity and interaction terms of Mb have been generated by using the DLGEN utility embedded in the DL\_PROTEIN package. The only modification to the standard Charmm22 force field that we have adopted has been the elimination of the C–O–Fe–N<sub>pyrrolic</sub> dihedral potential on the active site of Mb, since this contribution is ill defined for a quadrupole of atoms with three of them often lying on a line, as for the C–O–Fe triplet [18].

The system has been simulated within periodic boundary conditions with a proper treatment of electrostatics. The long-range nature of the Coulomb potential can be handled by the *ad hoc* Ewald summation method [19,20]. A very efficient strategy to compute electrostatics within this framework is the real-space implementation known as the smooth particle mesh Ewald (SPME) method [21], a numerical technique extremely efficient in its parallel implementation. The Ewald method has been used with an  $\alpha$  switching parameter of 0.31817 and the SPME method used  $30 \times 30 \times 30$  grid points and a spline order of 8.

All nonbonding interaction terms have been cutoff beyond a distance of 9 Å, with a shifted potential Van der Waals interaction and further smoothed by a polynomial switching function in the range of 0.5 Å before the cutoff.

The Mb+ solvent system has been simulated in the isobaric-isothermal (*NPT*) ensemble by using the Nosé-Hoover style equations of motion [22] where the volume of the system is allowed to fluctuate in an isotropic way. Coupling between the coordinates and momenta and the thermostatting and barostatting variables has been used with characteristic times of 0.5 and 5.0 ps, respectively, and the external pressure fixed at 1 atm.

We adopted a time-reversible extension of the velocity Verlet algorithm to integrate in time the equations of motion [23] by using a single time step scheme with a integration time of 2 fs. All chemical bonds of our system have been treated with holonomic constraints (in particular, the water model is treated as a rigid body). All constraints have been satisfied by using the shake iterative procedure [24], with modifications in the *NPT* ensemble, as described in [23].

The simulations presented here are part of a simulation protocol applied to study Mb in a wide range of temperatures, from 80 to 300 K, whose results will be published elsewhere. For each studied temperature we equilibrated the system for a period lasting about  $\approx 30$  ps depending on the considered temperature. In the equilibration protocol we have run the system with different procedures (such as the Berendsen and Nosé-Hoover equations of motion) in order to accelerate the equilibration phase. Once the potential energy and volume of the system have shown a stationary behavior we have begun the true equilibrium run, with configurations dumped each 0.1 ps over a total simulation time of 220 and 230 ps at 80 and 200 K, respectively.

The dynamic incoherent structure factor has been obtained by first computing the self-part of the intermediate scattering function, defined as

$$I(q,t) = \frac{1}{N} \sum_{i=1}^N \langle \exp[i\mathbf{q} \cdot \mathbf{r}_i(t)] \exp[-i\mathbf{q} \cdot \mathbf{r}_i(0)] \rangle, \quad (1)$$

where the sum runs over the class of atoms taken into account and  $N$  is the number of atoms of the given class. In particular, we have divided the protein into different shells and in the backbone and side chain atoms (as described in the next section). The positions of the protein atoms have been subtracted by spurious rototranslation contributions with the procedure described in [25], in order to observe only the protein intrinsic dynamic contribution to the spectra. The  $I(q,t)$  has been averaged over ten different directions of the vector  $\mathbf{q}$  in order to achieve a spherically averaged quantity, as experimentally measured. The intermediate scattering function has been computed for a total correlation time of 25.6 ps, and Fourier transformed in time to obtain the incoherent dynamic structure factor  $S_{inc}(q,\omega)$  and symmetrized by the factor  $\exp[-(\hbar\omega/2k_B T)]$  to satisfy detailed balance. The time correlation functions have been Fourier transformed without introducing any filtering procedure. Artifacts or aliasing effects due to the finite time correlation length have shown not to be significant in the part of the spectra under investigation.

## III. RESULTS AND DISCUSSION

Figure 1 reports the incoherent dynamic structure factor of myoglobin, calculated at a fixed  $q = 1 \text{ \AA}^{-1}$  and at two different temperatures, namely, 80 and 200 K, together with the one calculated from a previous simulation at 100 K [13] and the experimental data taken from the work of Diehl *et al.* at 150 K. The curve at 80 K in this plot has been rescaled to the reference temperature of 200 K upon the assumption that at 80 K the protein dynamics is harmonic. In this regime the

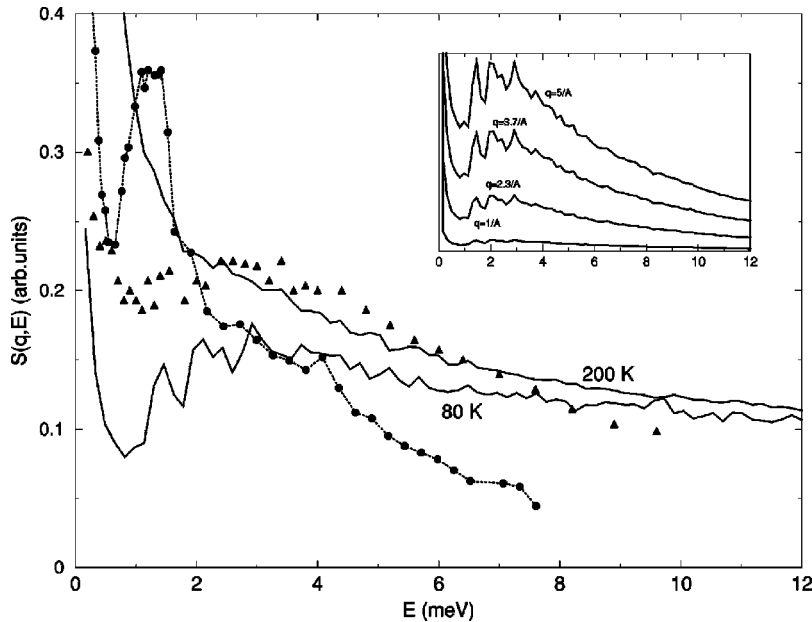


FIG. 1.  $S_{inc}(q, \omega)$  of Mb computed at  $q = 1 \text{ \AA}^{-1}$ . The scattering function at 80 K in this plot has been rescaled to the reference temperature of 200 K by multiplication by the Bose and Debye-Waller factors derived in the harmonic approximation as described in the text. The experimental data from Diehl *et al.* [12] for D<sub>2</sub>O-hydrated Mb (350 water molecules per protein) at 150 K are reported as triangles. The scattering function obtained from the MD data of Loncharich and Brooks [13] at 100 K and for Mb hydrated with 884 water molecules is also reported for comparison (full circles). Inset: unrescaled incoherent dynamic structure factor at 80 K at different scattering vectors.

spectrum may be rescaled to higher temperature by using the formula [8]

$$S_T^{harm}(q, \omega) = \frac{\hbar^2 q^2}{2m\omega} g(\omega) n(\omega, T) f(q, T), \quad (2)$$

where  $g(\omega)$  is the density of states,  $n(\omega) = 1/(\exp(\hbar\omega/k_B T) - 1)$  is the Bose factor,  $f(q, T) = \exp(-\langle \Delta x^2 \rangle_T q^2)$  is the Debye-Waller factor, and  $\langle \Delta x^2 \rangle = 1/3N \sum_i \langle \Delta r_i^2 \rangle$  is the isotropic average of the mean square displacement. The scattering function at 80 K has been upscaled by multiplying the calculated spectrum by the ratio  $S_{200}^{harm}(q, \omega)/S_{80}^{harm}(q, \omega) = n(\omega, 200)f(q, 200)/n(\omega, 80)f(q, 80)$ . The mean square displacements  $\langle \Delta x^2 \rangle_T$  are equal to 0.129 and 0.021  $\text{\AA}^2$  at 200 and 80 K, respectively, as computed for the nonexchangeable hydrogen atoms from the MD simulations. The obtained values differ by a factor of 3.4 and 2.3 from the experimental ones (0.038 and 0.009  $\text{\AA}^2$ ) at 200 and 80 K, respectively, as derived from the work of Doster *et al.* [6]. The ratio of the Debye-Waller factors are thus equal to 0.90 and 0.97 from simulations and experiments, respectively, at the scattering vector considered. However, it must be kept in mind that the scattering experiments were carried out at different temperatures and in a system less hydrated than in the simulations (350 and 1500 water molecules per atom in the experiments and in the simulations, respectively) implying that a direct comparison between the powders samples, as used in experiments, and the concentrated solution, as used in MD, must be considered with care as it will be discussed in the following of this paper.

Notwithstanding the above-mentioned differences the scattering function at 80 K shows a broadband centered at about 3 meV that reproduces in shape and energy the experimental one. Upon increasing the temperature the band is less resolved, as also experimentally found [5], because of the increasing intensity of a broad quasielastic contribution. The data show that the curves at 80 and 200 K overlap in the high-frequency regime, i.e., above  $\approx 10$  meV. The inset of Fig. 1 reports the  $q$  dependence of the scattering function at

80 K, which is found to be proportional to  $q^2$  for low  $q$ , as expected for incoherent scattering.

To our knowledge this is the first time that the low-frequency band calculated from a MD trajectory reproduces in shape and energy the experimental results; in fact, extensive simulations previously reported performed *in vacuo* and at different degrees of hydration were able to qualitatively reproduce the neutron scattering spectra but a shift toward lower frequencies of 1.2–2.5 meV was always observed [13,14] as it is shown by the curve represented by full circles in Fig. 1, which represent the  $S_{inc}(q, \omega)$  calculated from a previous MD simulation [13]. The reason for such a discrepancy was attributed to a too soft force field and/or to the different boundary conditions used in the experiments (crystal powders for neutrons and hydrated or solvated samples for MD) and/or truncation of the electrostatic interactions [14]. Of these three possible causes, the absence of periodic boundary conditions corresponds to simulate a system at zero pressure, such that artifacts can be induced on the structural and dynamical properties of the protein. Concerning the electrostatics, the use of a truncated Coulombic interaction induces a fictitious structure and dynamics on the system [26] and, in particular, a typical shift to lower frequencies in the dynamic properties of proteins [27,28]. In this context the authors of [14] have tried to improve the quality of the computed spectra by using either a distance-dependent dielectric constant or a switched cutoff of the potential, but in all the investigated cases a complete agreement for the inelastic band could not be found.

In our simulations we used the standard Charmm22 force field together with full electrostatics and the *NPT* ensemble to establish the proper density in order to assess if the mismatch with the experimental spectra could be due to the inadequacy of the microscopic model itself. The presented results indicate that the reasons for the previous mismatch in the dynamical properties must not be found in the choice of the force field, but in the simulation conditions. On the other hand, we again observe a deviation of the mean square displacement by a factor of 3 between experiments and simu-

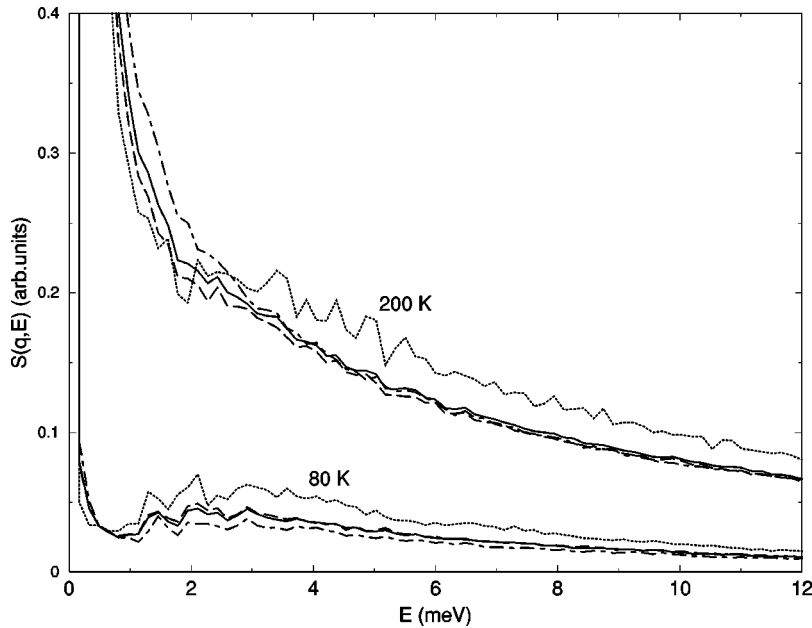


FIG. 2.  $S_{inc}(q=1 \text{ \AA}^{-1}, \omega)$  contributions from different shells of the hydrogen atoms belonging to the inner (dotted line), intermediate (dashed line), and external (dot-dashed line) shell. The weighted average over shells is also reported (solid line).

lations. This discrepancy is not cured by a full treatment of electrostatics and/or the use of periodic boundary conditions and it is likely to be due to the inaccuracy of the empirical force field.

The observed overdamping of the mean square displacements does not necessarily imply that the match of the hereby reported spectra with experiments is accidental, in particular, regarding the 3-meV band. In fact, based on the harmonic model as expressed by Eq. (2), the mean square displacements only enter the incoherent structure factor by rescaling globally the intensity of the spectra at given scattering vector. The approximation of a frequency-independent Debye-Waller factor has also been previously shown to hold for proteins in the range of temperatures under investigation [5]. Therefore, a correction of the microscopic model that reproduces the true ruggedness of the potential surface would eventually rescale the intensity and unlikely shift the 3-meV band, as it corresponds to slow and delocalized modes (15–25-ps timescale).

The use of the Nosé-Hoover equations of motion to sample the isobaric-isothermal ensemble could in principle affect the time-dependent properties of the systems, and presumably those of the protein itself, due to the coupling between the system positions and momenta with the piston and thermostat degrees of freedom. In order to test the quality of the computed dynamic properties we have carried out a simulation of Mb in the microcanonical ensemble (NVE) at 80 K for 150 ps, and at the same density as obtained in the  $NPT$  ensemble. The scattering function evaluated from this simulation superimposes remarkably well with the one obtained in the  $NPT$  ensemble, thus excluding the occurrence of dramatic artifacts in the  $S_{inc}(q, \omega)$  in the range of frequencies under investigation ( $>1$  meV) even by using a piston coupling time of 5 ps ( $\approx 0.8$  meV).

In order to elucidate the origin of the broadband at 3 meV and its possible relation with the surrounding solvent we have carried out an analysis of the MD data distinguishing protons belonging to the interior, intermediate, and external regions of the protein. To this purpose the protein has been divided into three shells comprised in the radii  $\{0.0, 8.2\}$  Å

for the first shell,  $\{8.2, 16.5\}$  Å for the second shell, and beyond 16.5 Å for the third shell. The inner, intermediate, and external shells contain 106, 546, and 352 nonexchangeable hydrogen atoms, respectively. The choice of the radii was made in order to avoid as much as possible the presence of solvent-accessible atoms in the intermediate and inner shells. On the other hand, each shell contains a substantial amount of both the backbone and side chain atoms. The scattering function of the protons from the inner, intermediate, and external shell evaluated at 80 and 200 K are reported in Fig. 2 without any rescaling to a common temperature. The reported  $S_{inc}(q, \omega)$  for each shell is an intensive quantity as defined by Eq. (1). This implies that the plot of Fig. 2 reports the contribution to the spectrum per hydrogen atom and the total scattering function reported therein is a weighted average of the shell's spectra.

It is interesting to notice that at 80 K the protons from the external shell contribute mostly to the ultralow modes  $E < 1$  meV while the protons of the inner region, i.e., the ones far away from the solvent, provide a contribution larger than those of the external and intermediate regions for  $E > 1$  meV. Such a result correlates well with the experimental findings that at low temperature a dry myoglobin sample (related to our inner core) exhibits a larger inelastic scattering at  $\approx 3$  meV than the hydrated one (related to our external shell) [12]. Moreover, the experimental result that dry Mb does not exhibit a large shift of the low-frequency band validates the comparison of the spectra obtained from simulation of a hydrated sample with the experimental one obtained on a sample having a lower degree of hydration.

At 200 K a broad, poorly defined band at around 3 meV arises equally from the protons of all shells. When considering the quasielastic region at  $E < 2$  meV, the external protons, i.e., those in contact with the solvent, provide a stronger scattering that almost completely masks the inelastic contribution at higher frequencies, similarly to the experimental data indicating that at high temperature the dry sample shows smaller quasielastic scattering than the  $D_2O$  hydrated sample [12]. At 200 K the high-frequency contribution of the inner



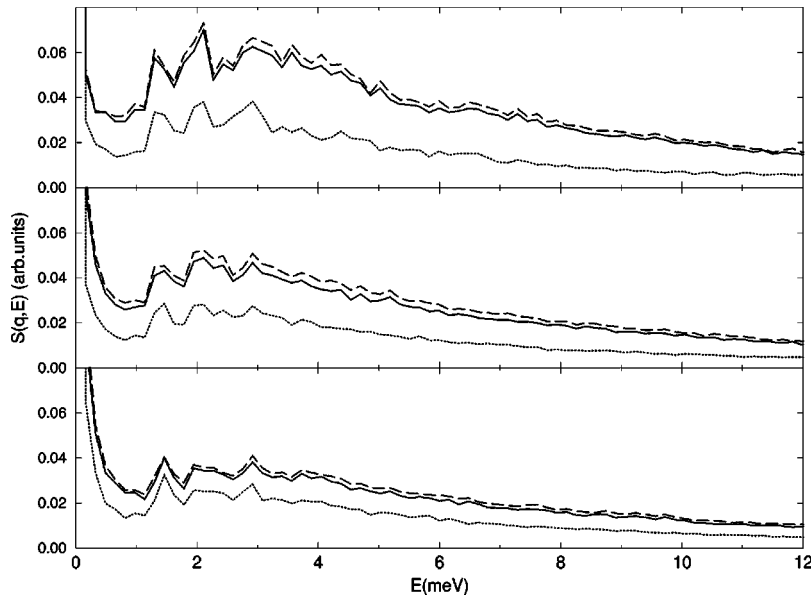


FIG. 3.  $S_{inc}(q=1 \text{ \AA}^{-1}, \omega)$  of the hydrogen atoms belonging to the backbone (dotted lines), side chain (dashed lines), and backbone+side chain (solid lines), evaluated for the inner (upper panel), intermediate (central panel), and external shell (lower panel) respectively, at 80 K.

and external shells cross above  $\approx 3$  meV where the high-frequency contribution from the inner part becomes predominant, in agreement with the experimental data that show an overdamping of the hydrated sample in the high-frequency range.

In order to better investigate the contribution of the different atoms belonging to the three above-mentioned shells, the  $S_{inc}(q, \omega)$ , separately calculated for the backbone and side chain nonexchangeable hydrogens at 80 and 200 K, have been reported in Figs. 3 and 4, respectively. The curves show that in each shell the side chain atoms contribute mostly to the spectra in all the frequency range and at both temperatures, in agreement with previous MD results on Mb at 300 K [29]. Moreover, the backbone and side chain atoms show similar characteristic frequencies, even when considering the fine structure of the spectrum, with a difference only in the relative amplitudes. From the data we observe that the side chain and backbone contributions to the total scattering function is shell and temperature dependent. The ratios of the intensities contributed by the side chain and the backbone

evaluated around 3 meV was found to be 1.9, 1.8, and 1.4 at 80 K and 2.0, 2.0, and 1.7 at 200 K, for the internal, intermediate, and external shells, respectively.

The backbone hydrogens at 80 K have a similar behavior in all the considered regions with a low-amplitude minimum at  $\approx 1$  meV, culminating in an inelastic peak at  $\approx 3$  meV, comparable in intensity. The contribution of the side chain atoms is strongly shell dependent, decreasing in intensity for  $E > 1$  meV when going from the internal to the external shell. Moreover, a transfer of modes from the inelastic peak to the lower-frequency region is visible when going from the internal to the external shells.

The differential contribution of the side chains belonging to the three shells indicates that the interaction of the external side chain atoms with the solvent decreases the intensity of the 3-meV band. Such a damping effect could be solely addressed to the soft electrostatic and hydrogen bond interactions that occur between the external polar side chain and water, as already suggested from the neutron scattering investigation [12].

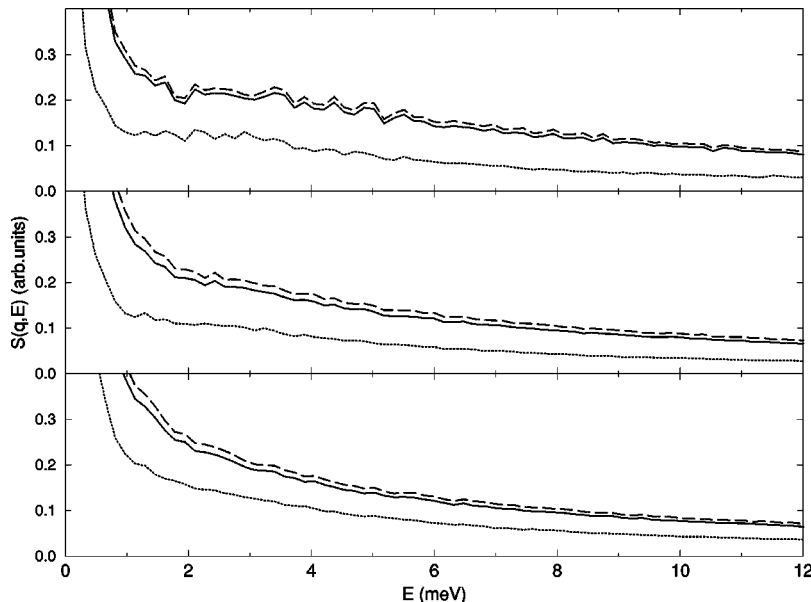


FIG. 4.  $S_{inc}(q=1 \text{ \AA}^{-1}, \omega)$  as in Fig. 3 but at 200 K.

Previous MD simulations on Mb [14] showed that the inelastic peak was damped and shifted to higher frequencies upon increasing the hydration level. The authors suggested that the icelike arrangement of the solvent inhibited the protein global motion. In our case we do not observe any frequency shift of the 3-meV band on going from the internal to the external shell, i.e., from a dehydrated to a hydrated environment. On the other hand, the presence of water produces a local damping of the side chain aminoacids located on the external region of the macromolecule, indicating that the damping effect due to hydration is a truly electrostatic effect, influencing the protein atoms in contact with the solvent. In fact, our results indicate that the presence of water produces a local damping on the side chain displacement of the amino acids located on the external region of the macromolecule. The different strength of the intraprotein versus protein-water hydrogen bonds is likely to be responsible for the observed behavior, since the contribution to the spectrum is strictly related to the accessibility of the amino acids to the solvent. Our study unambiguously indicates the existence of underdamped delocalized low-frequency modes associable to the internal matrix of the protein as partially predicted by normal mode analysis [9].

At 200 K the backbone hydrogens still exhibit some vague reminiscence of the inelastic peak at  $\approx 3$  meV, particularly in the inner shell. The high-frequency motion looks quite independent on the shell while the quasielastic contribution is larger in the external than in the inner shell. Similarly to the behavior observed at 80 K a transfer of modes from the high- to the low-frequency region when going from the internal to the external shell is again observed. At 200 K the contribution of the side chain and backbone atoms is more similar among shells than at 80 K. Such a similarity could be either a thermal effect intrinsic to the protein or may reflect a more complex interplay between the protein and the solvent.

#### IV. CONCLUSIONS

Our results indicate that the band at around 3 meV observed in several proteins is mainly contributed by the hydrogen atoms of the lateral chains of the protein inner region, while the ultralow modes are due mostly to the external shell. Such a phenomenon is evident at 80 K and can be interpreted by considering the existence of collective modes contributed by the lateral chains buried from the solvent. The contribution to the peak at 3 meV is damped and transferred to ultralow frequencies upon going from the internal to the external shell, because of the interaction between the external amino acids and the solvent. Such a damping effect was described by a previous MD simulation of Mb as a function of hydration [14] and was experimentally detected by a neutron scattering study on hydrated and dehydrated Mb [12]. At 200 K when the solvent around the protein has already melted in a supercooled liquid state [30], the inelastic region is equally contributed by all shells while prevalent low and ultralow modes from the side chain of the external shell are observed, again exhibiting the solvation effect.

In conclusion, MD data show that the inelastic band is due to soft modes intrinsic to the protein in itself, which prevail in the inner core. Experiments can be designed in order to highlight this effect in proteins of a different size and a different degree of hydration.

#### ACKNOWLEDGMENTS

The work of Maddalena Venturoli and Marco Pierro is warmly acknowledged in coding the topology builder program and preparing the input data for the simulations. We are grateful to Giovanni Ciccotti for a critical reading of the manuscript and to Carlo Pierleoni for many stimulating discussions. One of us (S.M.) wishes to thank Stefano Cozzini and Georges Destree for help with the development of DL\_PROTEIN. Finally, we wish to thank the supercomputing center Cineca (Bologna, Italy) for providing us with CPU time and support necessary for the accomplishment of this project.

- 
- [1] K. Brown, S. Erfurth, E.W. Small, and W.L. Peticolas, *Proc. Natl. Acad. Sci. USA* **69**, 1467 (1972).
  - [2] P. Painter, L. Mosher, and C. Rhoads, *Biopolymers* **21**, 1469 (1982).
  - [3] L. Genzel *et al.*, *Biopolymers* **15**, 219 (1997).
  - [4] S. Cusack, *Chem. Scr.* **29A**, 103 (1989).
  - [5] S. Cusack and W. Doster, *Biophys. J.* **58**, 243 (1990).
  - [6] W. Doster, S. Cusack, and W. Petry, *Nature (London)* **337**, 754 (1989).
  - [7] K.D. Moeller *et al.*, *Biophys. J.* **61**, 276 (1992).
  - [8] M. Bée, *Quasielastic Neutron Scattering* (Hilger, Bristol, 1988).
  - [9] Y. Seno, and N. Go, *J. Mol. Biol.* **216**, 111 (1990).
  - [10] N. Go, *Biopolymers* **17**, 1373 (1978).
  - [11] K.C. Chou, *Biophys. J.* **48**, 289 (1985).
  - [12] M. Diehl, W. Doster, W. Petry, and H. Schober, *Biophys. J.* **73**, 2726 (1997).
  - [13] R.J. Loncharich and B.R. Brooks, *J. Mol. Biol.* **215**, 439 (1990).
  - [14] P.J. Steinbach, R.J. Loncharich, and B.R. Brooks, *Chem. Phys.* **158**, 383 (1991).
  - [15] S. Melchionna, M. Falconi, and A. Desideri, *J. Chem. Phys.* **108**, 6033 (1998).
  - [16] S. Melchionna and S. Cozzini, DL\_PROTEIN 1.2 User Manual, 1997. DL\_PROTEIN has been developed from DL\_POLY for the simulation of proteins by the Italian Institute for the Physics of Matter under the Network on "MD simulation of biosystems," group University of Rome La Sapienza. DL\_POLY is a package of molecular simulation routines written by W. Smith and T. R. Forester, copyright—The Council for the Central Laboratory of the Research Councils, Daresbury Laboratory at Daresbury, Nr. Warrington, 1996.
  - [17] A.D. MacKerell *et al.*, *J. Phys. Chem. B* **102**, 3586 (1998).
  - [18] M. Venturoli and G. Ciccotti (unpublished).
  - [19] M. P. Allen and D. J. Tildesley, *Computer Simulation of Liquids* (Clarendon, Press, Oxford, 1987).
  - [20] J.-P. Hansen, in *Molecular Dynamics Simulation of Statistical-Mechanics Systems*, edited by G. Ciccotti and W. G. Hoover (SIF, Como, Italy, 1986).

- [21] U. Essmann *et al.*, *J. Chem. Phys.* **103**, 8577 (1995).
- [22] S. Melchionna, G. Ciccotti, and B.L. Holian, *Mol. Phys.* **78**, 533 (1993).
- [23] G.J. Martyna, M.E. Tuckerman, G.J. Tobias, and M.L. Klein, *Mol. Phys.* **87**, 1117 (1996).
- [24] G. Ciccotti and J.P. Ryckaert, *Comput. Phys. Rep.* **4**, 345 (1986).
- [25] G.R. Kneller, *Mol. Simul.* **3**, 271 (1989).
- [26] J. Madura and B.M. Pettitt, *Chem. Phys. Lett.* **150**, 105 (1988).
- [27] J.C. Smith, S. Cusack, B. Tidor, and M. Karplus, *J. Chem. Phys.* **93**, 2974 (1990).
- [28] J.C. Smith, *Q. Rev. Biophys.* **24**, 227 (1991).
- [29] G.R. Kneller and J.C. Smith, *J. Mol. Biol.* **242**, 181 (1994).
- [30] M. Pierro, S. Melchionna, and M. Venturoli (unpublished).